Microscopic Constitutive Equation Theory for the Nonlinear Mechanical Response of Polymer Glasses

Kang Chen and Kenneth S. Schweizer*

Department of Materials Science and Engineering, University of Illinois, 1304 West Green Street, Urbana, Illinois 61801

Received April 7, 2008; Revised Manuscript Received June 3, 2008

ABSTRACT: Building on recent statistical mechanical theories of segmental activated barrier hopping and elasticity in quiescent and stressed polymeric materials, we construct a constitutive equation description at a generalized Maxwell model level for the nonlinear mechanical response of polymer glasses. The key physics is contained in a deformation-dependent elastic modulus and alpha relaxation time. Calculations of the temperature and strain rate dependence of the stress−strain curves, yield stress, and yield strain are presented for atactic poly(methyl methacrylate) (PMMA). The strain rate dependences of these properties are roughly logarithmic with upward deviations at very high rates. Yield stresses grow approximately linearly as temperature is lowered. Stress−strain curves at different temperatures and strain rates can be collapsed onto a master curve based on nondimensionalizing stress by the plateau yield stress and strain by an effective critical strain. Quantitative comparisons of the theory with several experimental measurements of the elastic modulus and stress−strain response of PMMA glasses reveal good agreement. Predictions are also made for how deformation reduces the segmental relaxation time. In the plastic flow regime a "shear thinning" type of dependence of the alpha time on strain rate occurs corresponding to an effective power law decay with strain rate. Proper nondimensionalization results in a master curve that collapses the temperature dependence. In the dynamic yielding regime the segmental relaxation time is predicted to be (much) shorter than the inverse strain rate. Hence, our results provide theoretical support for the qualitative idea that stress-induced local plastic flow can be thought of as a "devitrification transition". The implication of our results for the question of beyond what length scale a polymer glass deforms affinely is briefly addressed.

I. Introduction

Theoretical understanding of the ultraslow dynamics and mechanical properties of polymer glasses is a challenging problem of fundamental scientific interest and high technological importance.[1−5] Below the kinetically defined glass transition temperature, T_g, equilibration is often not experimentally accessible due to the explosive growth of relaxation times with cooling. However, under the influence of external deformation the segmental scale (alpha) relaxation time can be greatly reduced resulting in irreversible *local* "plastic flow" or "dynamic yielding". The latter terminology defines a dynamical state where segmental relaxation occurs on the experimental time scale. Polymers are not ideal plastic materials since their yield stress is a strong function of temperature and deformation rate.[3−9] Hence, yielding is fundamentally a viscous process, often described as a mechanically assisted solid-to-liquid or "devitrification" transition[3] that occurs at strain amplitudes of ∼5−10%. Mechanical measurements have inferred a massive reduction of the relaxation time with stress,[10] and more direct experiments[11,12] and computer simulations[13−18] have observed accelerated segmental motion.

Because of the complexity of the problem, the phenomenological Eyring model[4,5,19] is still widely employed as a conceptual framework for describing dynamic yielding in polymer glasses. This model assumes the mean alpha relaxation time, τ_α, reflects a simple Arrhenius activated hopping process (characterized by a single *potential* energy E_A) of an undefined elementary unit. Applied stress (τ) results in a *linear* reduction of the barrier of a mechanical work form:[5,19]

$$\tau_\alpha(T,\tau) = \tau_0 \exp[(E_A - \tau V^*)/k_B T] \quad (1)$$

where k_BT is the thermal energy, τ_0 is a vibrational time scale, and V^* is an empirical, temperature-*independent* "activation volume". A "plastic strain rate", $\dot{\gamma}_{pl} \propto \tau_\alpha^{-1}$, is often introduced. A *dynamic* yield stress, τ_y, is identified as when the externally imposed strain rate ($\dot{\gamma}$) is of order the thermal hopping rate

$$\tau_\alpha(T,\tau_y) = a\dot{\gamma}^{-1} \quad (2)$$

where "a" is a numerical factor of order unity. Equations 1 and 2 then result in an explicit expression for the dynamic yield stress which for $a = 1$ is given by

$$\tau_y = \frac{E_A}{V^*} + \frac{k_B T}{V^*} \ln(\dot{\gamma}\tau_0) \quad (3)$$

Equation 3 predicts (i) the rate-independent contribution is a temperature-independent material constant, (ii) the temperature and strain rate dependences enter in a multiplicative fashion, and (iii) τ_y grows linearly with temperature and logarithmic strain rate.

Experimental[3−5] and simulation[20] studies have raised serious concerns about the validity of several aspects of the Eyring model and its ability to identify intrinsic material parameters. For example, (a) the extracted values of V^* vary enormously (∼1−20 nm^3) with no apparent correlation with structural properties, (b) empirical fits to data often require the counterintuitive trend that V^* increases with heating, (c) the extracted "constant" activation volume shows a dependence on stress and strain, (d) over 2−3 orders of magnitude in strain rate the yield stress is linear in ln ($\dot{\gamma}$), but a systematic upward curvature occurs at high rates, (e) the strain rate dependence of τ_y does *not* become weaker upon cooling, but rather is nearly temperature independent or gets stronger, and (f) the leading rate-independent contribution to τ_y is *not* temperature independent as in eq 3, but rather increases with cooling in an initially linear manner with upward curvature at lower temperatures.

Computer simulations of model glassy polymers that address segmental relaxation and the effect of applied stress have been

* Corresponding author. E-mail: kschweiz@uiuc.edu.

10.1021/ma800778v CCC: $40.75
Published on Web 07/15/2008

recently performed.[13–18,20] A key finding is that the time dependence of macroscopic quantities (e.g., creep compliance) is strongly correlated with microscopic activated motions on a *small* length scale as quantified, for example, by the segmental mean-square displacement or incoherent dynamic structure factor on the cage scale.[13] Moreover, despite the globally anisotropic nature of mechanical tests (extension, compression, shear), the dynamics on the segmental scale is very nearly *isotropic*.[13,15] These somewhat surprising aspects are qualitatively identical to what has been found in experiments on glassy colloidal suspensions[21] and simulations of simple atomic mixture models[22,23] and represent welcome simplifications in the search for a predictive theory.

Recently, Saltzman and Schweizer have constructed a force level theory for segmental activated barrier hopping dynamics in cold polymer melts[24–26] based on earlier work for colloidal suspensions and hard sphere fluids.[27–29] The approach was generalized by the present authors to the quiescent nonequilibrium glass state in the absence[30] and presence[31] of physical aging. The polymer glass theory has been extended to treat elementary consequences of applied stress on the alpha time and yielding phenomenon.[32] The predictions of that theory were shown to be qualitatively consistent with prior[3–5] and recent[12] experiments and are also in accord with a recent simulation[15] of stress-accelerated segmental dynamics.

The purpose of the present paper to develop a constitutive equation theory for the mechanical response of deformed polymer glasses built on our recent advances. We invoke several simplifying assumptions since our initial goal is to create a minimalist analytic description. Specifically, the coupled phenomena of physical aging and deformation-induced "rejuvenation"[2,3,33] will be ignored. This simplification is realizable in mechanical experiments carried out immediately after rapid quenches or after a mechanical "pretreatment".[3–5,7] We only consider the mean alpha relaxation process. This implies a Maxwell-like model description of stress relaxation and the neglect of dynamical fluctuation or heterogeneity effects[34] associated with nonexponential relaxation.[1] The large deformation regime where the distinctly polymeric phenomenon of "strain hardening"[3–5,35] emerges is also not addressed. All these aspects are under active study as will be reported in future publications.

In section II we summarize the relevant elements of prior work. Model calculations are presented for poly(methyl methacrylate) (PMMA) melts and glasses in section III, which is the representative amorphous polymer material chosen to illustrate the predictions of the theory. A general constitutive equation model is developed and discussed for constant strain rate experiments in section IV. Section V presents numerical applications of the theory, including quantitative comparisons to PMMA experiments. Calculations for the effect of deformation on the segmental relaxation time are given in section VI. The paper concludes in section VII with a discussion and summary.

II. Theory for Supercooled Melts and Glasses

In this section we summarize the essential aspects of the relevant prior theories for relaxation in quiescent and stressed polymer melts[24–26] and glasses[30–32] which are input to the new constitutive equation theory.

A. Quiescent Supercooled Melts. The segmental activated barrier hopping theory in cold polymer melts[24–26] and glasses[30,31] is built on a locally solid-state picture of slow dynamics. A microscopic statistical mechanical derivation for glassy atomic liquids and particle suspensions has been achieved.[28] The polymer melt is dynamically treated as a liquid of coarse-grained "statistical segments" of size σ.[24] The explicit *dynamical* effects of chain connectivity are neglected which is qualitatively consistent with the independence for long chains of glassy relaxation and initial yielding on degree of polymerization.[3–5] The instantaneous scalar *displacement* of a segment from its initial ($t = 0$) position, $r(t)$, obeys a nonlinear stochastic Langevin equation of motion:

$$-\zeta_s \frac{\partial r(t)}{\partial t} - \frac{\partial F_{\rm eff}(r(t))}{\partial r(t)} + \delta f(t) = 0 \qquad (4)$$

where the white noise random force satisfies $\langle \delta f(0)\delta f(t)\rangle = 2k_BT\zeta_s\delta(t)$, and $\zeta_s = k_BT/D_s$ is the short time friction constant associated with the fast and very local dynamic process. The effective "nonequilibrium free energy" consists of a translational entropy contribution which favors the fluid state and an *interchain* caging force contribution which favors segment localization and the glass state:

$$\frac{F_{\rm eff}(r)}{k_BT} = -3\ln(r) - \int \frac{d\vec{q}}{(2\pi)^3}\rho C^2(q)S(q)[1+S^{-1}(q)]^{-1} \times \exp\left\{-\frac{q^2r^2}{6}[1+S^{-1}(q)]\right\} \qquad (5)$$

For long Gaussian polymer "thread" chains[24] the site−site direct correlation function is wavevector-independent $C(q) = C_0$, and the inverse collective density fluctuation structure factor is $S^{-1}(q) = S_0{}^{-1} + q^2\sigma^2/12$. In equilibrium $S_0 \equiv S(q{=}0) = \rho k_BT\kappa = (-\rho C_0)^{-1}$ is the dimensionless compressibility which quantifies the amplitude of nanometer and larger scale density fluctuations. The statistical segment length that enters the *equilibrium* single chain structure factor is $\sigma = C_\infty{}^{1/2}l$, where l is the average length of a backbone chemical bond and C_∞ is the characteristic ratio, and $\rho\sigma^3$ is the reduced segmental density which is of order unity. A simple temperature dependence for S_0 describes experimental data extremely well: $S_0{}^{-1/2} = -A + (B/T)$, where $A > 0$ and $B \sim 10^3K$ is proportional to the melt cohesive energy.[24] The key ideas underlying eqs 4 and 5 are to use dynamic density functional methods at the dynamical variable level, in conjunction with a local equilibrium picture and a self-consistent approximate relation between one- and two-particle dynamics.[28]

For long chains a single material parameter or "coupling constant" determines $F_{\rm eff}(r)$: $\lambda \equiv (\rho\sigma^3S_0{}^{3/2})^{-1}$. This parameter increases with cooling[24] and is computable from *experimentally measurable* static properties, which is the origin of the predictive power of the approach. Below a theoretically computed *dynamic crossover* temperature, T_c, $F_{\rm eff}(r)$ acquires a localization well and *temperature-dependent* barrier $F_B(T)$. Above T_c the relaxation time is treated in an Arrhenius form: $\tau_0(T) \equiv \tau_0 \exp(\varepsilon/k_BT)$, where $\tau_0 \simeq 10^{-14}$ s and ε is a local activation energy determined from the experimental observation[36] that $\tau_0(T_c) \cong 10^{-7}$ s.

A literal interpretation of the "segmental liquid" model is that chain connectivity does not modify the barrier hopping process. In reality, there are short-range equilibrium correlations along the polymer backbone which must have *quantitative* dynamic consequences. To model this aspect, a temperature-*independent* "cooperativity parameter", a_c, is introduced which leads to an effective barrier[24–26] height of a_cF_B. Physically, a_c corresponds to the number of dynamically correlated segments along the chain. A dynamical intrachain correlation length is typically estimated from a measure of backbone stiffness: either the Kuhn length $l_k = C_\infty l$ or persistence length $\xi_p = (C_\infty + 1)l/2$.[37,38] For the Gaussian chain model the cooperativity parameter can be estimated by equating the end-to-end distance of the dynamically cooperative unit ($a_c{}^{1/2}\sigma$) to the Kuhn or persistence length, thereby yielding $a_c = C_\infty$ or $a_c = (C_\infty + 1)^2/4C_\infty$, respectively. Since typically $C_\infty \approx 4{-}10$, estimates of $a_c \sim 1{-}10$ follow.

Combining all the above elements, the segmental hopping (alpha) time that smoothly bridges the Arrhenius and deeply supercooled regimes is given by[24]

$$\tau_\alpha(T) = \tau_0 \exp(\varepsilon/k_BT) \exp(a_c F_B(T)/k_BT) \quad (6)$$

The kinetic glass temperature is defined by $\tau_\alpha(T_g) = 10^2-10^4$ s. The ability of the theory to compute the temperature-dependent barrier, $F_B(T)$, from the experimental knowledge of the melt density and compressibility is the origin of its demonstrated predictive power for understanding the temperature dependence of the segmental alpha time, glass transition temperatures, dynamic fragilities, and other properties of cold polymer melts.[24–26] It serves as a generic description of any measurement that probes the alpha relaxation process. Of course, different experiments, such as NMR, dielectric, and mechanical measurements, probe quantitatively different aspects of the alpha process. However, the characteristic relaxation times are often quantitatively close and follow nearly identical temperature dependences.[1]

B. Glasses. Below T_g the fundamental aspects of the theoretical approach are assumed to still apply.[30] However, as discussed theoretically[30,39,40] and experimentally,[41–45] the equilibrium statistical mechanical relationship $(-\rho C_0)^{-1} = S(q=0) = \rho k_B T \kappa$ between the amplitude of density fluctuations, and the isothermal compressibility no longer holds. The physical reason is that dynamic interconversion between different liquid packing structures becomes very slow below T_g, resulting in a frozen-in component of density fluctuations. In more modern language, the "effective temperature" associated with the configurational (not vibrational nor fast relaxation process which remain equilibrated) degrees of freedom is higher than the physical temperature.[39,46] To determine the coupling constant λ, the results of scattering measurements and elementary landscape concepts have motivated a simple additive description of the structural and phonon-like contributions to the density fluctuation amplitude:[30]

$$S_0(T) \simeq bS_0(T_g) + (T/T_g)(1-b)S_0(T_g) \quad (7)$$

where $S_0(T\to 0) \equiv bS_0(T_g)$ quantifies the frozen component and for polymers $b \sim 0.4-0.75$.[30,41–45] The alpha relaxation time of eq 6 is *nondivergent* both above and below T_g. The theory predicts[30] Arrhenius-like relaxation in the nonequilibrium glass state consistent with measurements on many polymer glasses.[47–52]

C. Effect of Deformation. Stress-induced acceleration of segmental relaxation and dynamic yielding in polymer glasses has been discussed at an elementary level in our recent work.[32] The polymer theory builds on the successful approach of Kobelev and Schweizer for the alpha relaxation, elastic modulus, and yielding behavior of deformed colloidal glasses and gels.[53,54] An effectively isotropic approximation is adopted with stress inducing a constant external force on a tagged segment, $f = c\sigma^2\tau$. Here, consistent with our prior notation,[32,53] τ is the applied stress (not to be confused with the mean barrier hopping time, τ_α), and c is a numerical constant of order unity. The latter is determined[55] by the segmental cross-sectional area needed to convert stress to a force and is given by[32,53] $c = (\pi\rho\sigma^3/6)^{-2/3}$. The coupling constant λ is taken to be unmodified by deformation; i.e., stress does not change the glass density or the amplitude of density fluctuations. The fast and highly local relaxation process described by $\tau_0(T)$ is also assumed to be deformation independent. All these simplifications appear to be good first approximations based on experiments[4,5,33] and simulation studies.[13,22,23] For example, recent X-ray scattering studies have shown that even for significant deformations beyond the yield point the single chain ($\omega(q)$) and collective ($S(q)$) structure factors remain essentially isotropic on the segmental and cage length scales, and $S(q)$ is nearly isotropic beyond the nanometer scale.[56,57] Moreover, simulations of glassy polymers find segmental dynamics is accelerated by applied stress in an isotropic manner.[13–15] The idea that deformation does not modify the material properties that enter the coupling constant λ or $\tau_0(T)$ is consistent with the relevant segmental displacement length scale being small as suggested by computer simulations.[13–15]

Note that, in contrast to the Eyring approach,[19] stress enters at a microscopic *dynamic variable* level via distortion of the nonequilibrium free energy. This idea is equivalent to modeling deformation as a mechanical work type of contribution to $F_{eff}(r)$ which depends linearly on applied stress and *instantaneous* segment displacement:

$$-fr = -c\sigma^2\tau r \quad (8)$$

Application of this approach to predict dynamic yielding has been shown to be in semiquantitative accord with experiment.[32] The key idea that stress reduces the effective barrier to activated motion has fundamental support from potential energy landscape studies[58] and also is the centerpiece of the phenomenological "soft glassy rheology" approach.[59]

The glassy elastic shear modulus follows from the standard Green−Kubo formula as[30]

$$G' = \frac{k_BT}{60\pi^2}\int_0^\infty dq \left[q^2\frac{\partial}{\partial q}\ln S(q)\right]^2 e^{-q^2r_L^2/3S(q)} \quad (9)$$

where r_L is the local minimum, or transient localization length, of the nonequilibrium free energy, which grows with stress. Hence, the elastic modulus is reduced, or "softened", with applied deformation. Many mechanical tests involve compression or tension which are described by Young's modulus, E'. The latter is related to its shear analog as $E' = 2G'(1+\nu)$, where ν is Poisson's ratio. Experiments on polymer glasses find the Poisson ratio is a weak function of temperature.[60] For example, $\nu \sim 0.5$ near T_g and then decreases slowly and roughly linearly with further cooling. Typically, $E'/G' \sim 2.5-3$ over a range of temperatures below T_g. For simplicity, in our model calculations below we fix $\nu = 0.4$, or equivalently $E' \simeq 2.8G'$.

III. Model Calculations: Poly(methyl methacrylate) Melts and Glasses

As a prelude to the application of our constitutive equation theory, we present key results for atactic PMMA based on the theory outlined in section II. The PMMA compressibility and density data yield[24] above T_g the parameters $A \simeq 0.693$ and $B \simeq 1134$ K that quantify $S_0(T)$. The glass temperature is defined by $\tau_\alpha(T_g) = 100$ s. By requiring the theory reproduces[30] the typical experimental values of T_c (426 K) and T_g (378 K) in the equilibrated melt state, we deduce $\rho\sigma^3 = 0.92$ and $a_c \simeq 5$. Unless stated otherwise, the segment length is fixed at $\sigma = 1$ nm. It is significant to note that these values of segmental density, cooperativity parameter, and segment length are consistent with a priori estimates based on chain stiffness and melt density.[26,30] The theory predicts a dynamic fragility at T_g of ~130, in good accord with observations. In the glass state, the frozen density fluctuation parameter is fixed at $b = 2/3$, a value consistent with X-ray scattering experiments on PMMA.[44,45]

Figures 1 and 2 present a selection of results for PMMA. The main panel of Figure 1 shows the mean alpha relaxation time as a function of scaled inverse temperature at several different applied stress levels. Stress reduces the barrier and accelerates segmental relaxation. In the quiescent glass state an *effective* Arrhenius behavior is generically obtained, the details of which are in accord with multiple measurements.[30,47–52] The crossover to Arrhenius behavior also occurs

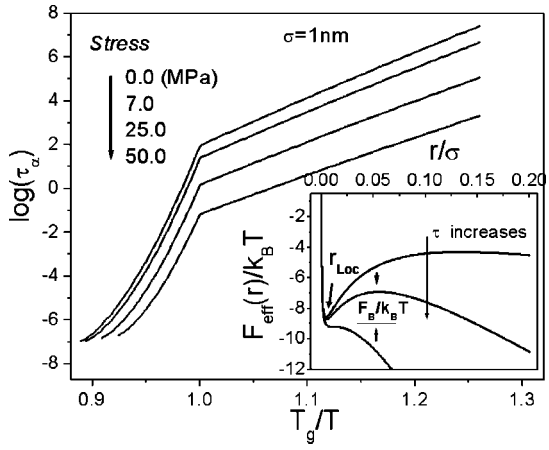

Figure 1. Logarithmic (base 10) segment relaxation time (seconds) as a function of inverse scaled temperature under quiescent conditions and at three nonzero stress levels. Inset: nonequilibrium free energy as a function of reduced segmental displacement for PMMA[30] at $T = T_g - 30$ K $= 348$ K and $b = 0.67$ for various stress levels. The localization length (r_{LOC}) and dimensionless barrier (F_B/k_BT) are depicted.

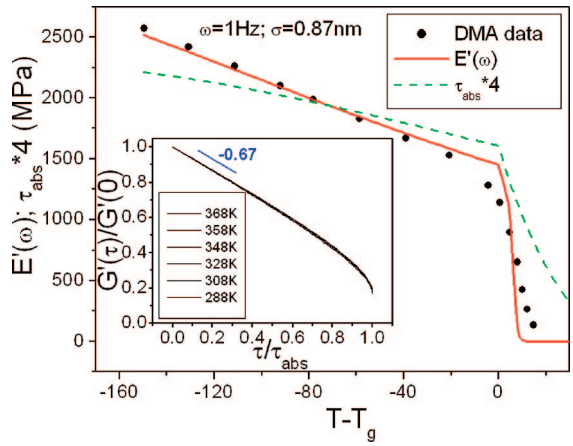

Figure 2. Dynamic component of Young's modulus at a frequency of 1 Hz, $E'(\omega)$ (solid curve), and the absolute yield stress multiplied by four (dashed curve), in megapascals for PMMA as a function of degree of undercooling. Solid circles are the α process component of the experimental elastic modulus measured at 1 Hz.[8] The statistical segment length is 0.87 nm. Inset: master curve of the shear elastic modulus reduced by its linear response value as a function of stress reduced by its (temperature dependent) absolute yield value for several temperatures covering the range from 10 to 90 K below T_g. A linear fit to the regime of $\tau/\tau_{abs} \ll 1$ yields a slope of -0.67.

under stress with the only difference being that the corresponding value of relaxation time and apparent activation energy decrease. The inset of Figure 1 shows an example of the deformed nonequilibrium free energy, $F_{eff}(r;\tau)$. With increasing stress the localization length (barrier) shifts weakly outward (strongly inward), and the barrier height decreases and ultimately vanishes at a critical value of stress called the "absolute yield stress",[32] τ_{abs}. Numerical calculations of the stress reduction of the barrier can be well described by a critical power law:[24,25]

$$F_B(\tau)/F_B(0) \cong (1 - \tau/\tau_{abs}(T))^{\upsilon} \tag{10}$$

where the apparent exponent $\upsilon \sim 2.5$.

Figure 2 presents calculations of linear and nonlinear mechanical properties. Results for the dynamic Young's modulus in the Maxwell model spirit, $E'(\omega) = E'(\omega\tau_\alpha)^2/[1 + (\omega\tau_\alpha)^2]$, are shown at a frequency of 1 Hz and are compared to PMMA experiments.[8] Rather good agreement is found between theory and experiment below T_g by choosing $\sigma = 0.87$ nm, the only adjustable parameter in the comparison. This value of segment length is sensible since it is intermediate between the persistence and Kuhn lengths of PMMA given by ~0.75 and 1.35 nm, respectively. The absolute yield stress increases roughly linearly with cooling below T_g. The inset of Figure 2 shows the reduction of the glassy elastic shear modulus (softening) with stress follows a universal behavior at different temperatures if it is normalized by the quiescent value and stress is nondimensionalized by the absolute yield stress. Note that at the absolute yield point ($\tau = \tau_{abs}$) the modulus is reduced by a factor of ~5−6. Dynamic yielding occurs[32] at applied stresses where typically the ratio $\tau/\tau_{abs} \ll 1$. Under this condition the universal master curve is well represented as a linear function of applied stress

$$G'(\tau) \simeq G'(0)\left(1 - \frac{2}{3}\frac{\tau}{\tau_{abs}}\right) \tag{11}$$

IV. Constitutive Equation Theory

We now propose a constitutive equation in the Maxwell model spirit which requires as input *only* an elastic modulus and mean alpha relaxation time. The contribution of the highly local and fast relaxation process to the mechanical response, and hence the "two-step decay" of a dynamic modulus, is thus ignored. This simplification has little consequences at the sub-T_g temperatures of interest. The key physics is deformation dependence of the elastic modulus and relaxation time which is described based on the approach of section II. Since we apply the theory in this paper to elongation and compression experiments, the formalism is developed in terms of Young's dynamic modulus, $E(t)$.

A. General Formulation. The starting point is the Boltzmann superposition principle. Assuming the applied deformation begins at time $t = 0$ one has

$$\tau(t) = \int_0^t E(t - t')\, \dot{\gamma}(t')\, dt' \tag{12}$$

where $\dot{\gamma}(t)$ is a time-dependent strain rate. In linear response $E(t)$ is independent of strain history. In the nonlinear regime we adopt eq 12 as a plausible ansatz by introducing a deformation-dependent relaxation modulus, $E(t;\tau(t))$, which obeys a first-order kinetic equation:

$$\frac{dE(t;\tau(t))}{dt} = -\frac{E(t;\tau(t))}{\tau_\alpha(\tau(t))} \tag{13}$$

Formally integrating eq 13 yields

$$E(t - t') = E'(\tau(t'))\, \exp\left\{-\int_{t'}^{t} dt''\, \tau_\alpha^{-1}[\tau(t'')]\right\} \tag{14}$$

where $E'(\tau) = 2.8G'(\tau)$ is the stress-dependent glassy elastic modulus. Equation 14 is of the classic "effective time" form.[2,33,61] Note that since stress history enters, $E(t)$ is not a strictly exponentially decaying function of time. Combining eqs 12 and 14 yields

$$\tau(t) = \int_0^t dt'\, E'(\tau(t'))e^{-\int_{t'}^{t} dt''\tau_\alpha^{-1}[\tau(t'')]}\dot{\gamma}(t') \tag{15}$$

Equations 5–9 and eq 15 comprise a self-consistent, highly nonlinear description of mechanical response. The time-local, generalized Maxwell differential form follows from differentiating eq 15 with respect to time

$$\frac{d\tau}{dt} + \frac{\tau}{\tau_\alpha(\tau)} = E'(\tau)\, \dot{\gamma}(t) \tag{16}$$

The corresponding viscosity is

$$\eta(\tau) = \int_0^\infty E(t;\tau)\, dt = E'(\tau)\, \tau_\alpha(\tau) \tag{17}$$

A special limit of interest is $\dot{\gamma}\tau_\alpha \to \infty$ corresponding to no thermally induced activated hopping on the mechanical experiment time scale. This limit can be interpreted as solid or "granular-like" in the sense that deformation is elastic until a critical stress is reached which triggers absolute yielding. The constitutive equation then becomes

$$\gamma = \int_0^\tau \frac{d\tau'}{E'(\tau')} \tag{18}$$

B. Constant Strain Rate Protocol. For a constant strain rate experiment the strain is given by $\gamma \equiv \dot{\gamma}t$. The stress−strain relation then follows from eq 15 as

$$\tau(\gamma) = \int_0^\gamma d\gamma'\, E'(\gamma') e^{-\int_{\gamma'}^{\gamma} d\gamma''/[\dot{\gamma}\tau_\alpha(\tau(\gamma''))]} \tag{19}$$

or in differential form

$$\frac{d\tau(\gamma)}{d\gamma} + \frac{\tau(\gamma)}{\dot{\gamma}\tau_\alpha(\gamma)} = E'(\tau) \tag{20}$$

Dynamic yielding, or plastic flow, corresponds to when $d\tau/d\gamma = 0$, a condition which determines the dynamic yield stress as

$$\tau_y = \dot{\gamma}(E'(\tau_y)\tau_\alpha(\tau_y)) = \eta(\tau_y)\dot{\gamma} \tag{21}$$

The language "dynamic yield" (or plastic flow) stress indicates flow occurs in an activated manner that depends on the external strain rate. In our previous work,[32] the Eyring-like dynamic yielding criterion of eq 2 was employed, $\tau_\alpha(\tau_y)\dot{\gamma} = 1$. This is a shear-thinning-like crossover condition that identifies yielding as when segments relax on the experimental time scale ($\dot{\gamma}^{-1}$). However, the constitutive equation predicts

$$\tau_\alpha(\tau_y)\dot{\gamma} = \tau_y/E'(\tau_y) \equiv \tilde{\gamma}_y \tag{22}$$

where $\tilde{\gamma}_y$ is referred to as an "effective yield strain". We show below that the product $\tau_\alpha(\tau_y)\dot{\gamma}$ is neither unity nor a temperature- and strain-rate-independent constant.

Useful analytic analysis of the dynamic yielding condition can be achieved. Using eqs 6, 10, and 11 in eq 21, one easily obtains

$$\frac{\tau_y}{\tau_{abs}} = \dot{\gamma}\frac{E'(0)}{\tau_{abs}}\left(1 - \frac{2\tau_y}{3\tau_{abs}}\right)\tau_0 \exp(\beta\varepsilon) \exp\left[\beta a_c F_B(0)\left(1 - \frac{\tau_y}{\tau_{abs}}\right)^{5/2}\right] \tag{23}$$

This is a nonlinear self-consistent equation for the dynamic yield stress which is a function of essentially all the temperature-dependent material parameters. To simplify, we introduce a dimensionless yield stress and an absolute yield strain variable of theoretical significance

$$\theta \equiv \frac{\tau_y}{\tau_{abs}}; \quad \tilde{\gamma}_{abs} = \frac{\tau_{abs}}{E'(0)} \tag{24}$$

Equation 23 can then be written as

$$\theta = \tilde{\gamma}_{abs}^{-1}(\dot{\gamma}\tau_\alpha(0))\left(1 - \frac{2}{3}\theta\right)\left(e^{\beta a_c F_B(0)}\right)^{(1-\theta)^{5/2}-1} \tag{25}$$

It is of interest to know the value of the product of the strain rate and relaxation time at *dynamic yielding*, $(\dot{\gamma}\tau_\alpha)_y$. If this quantity is much less than unity, the system can be thought of as equilibrated in a dynamical sense on the segmental scale under plastic flow conditions.

V. Mechanical Response at Constant Strain Rate

We now apply our constitutive equation theory to constant strain rate experiments on PMMA glasses. Our results are representative of other amorphous plastics such as polycarbonate and atactic polystyrene. The calculations are relevant to measurements carried out under rapid quenching conditions, or mechanical pretreatment, where physical aging and mechanical "rejuvenation" are largely absent and no macroscopic mechanical failure phenomena are present.[3,7] Calculations are performed for temperatures below T_g and strain rates typical of experiments. Note that all material parameters of the theory have been *fixed*, and hence the results should be viewed a predictions for PMMA glass properties devoid of adjustable fit parameters.

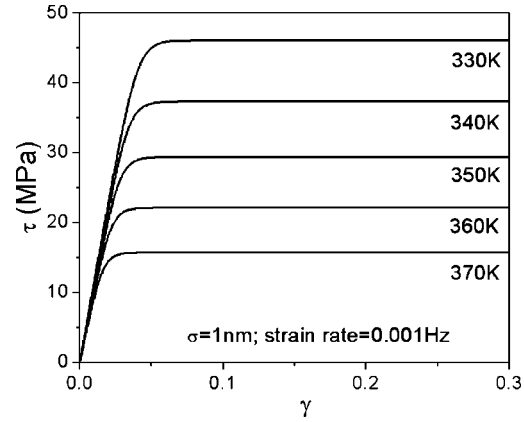

Figure 3. Stress−strain response of PMMA at a constant strain rate of 0.001 Hz for five temperatures.

A. Temperature Dependence. Figure 3 shows stress−strain curves at temperatures that vary from 8 to 48 K below T_g at a fixed strain rate of $\dot{\gamma} = 10^{-3}$ Hz. The stress initially rises linearly in the elastic regime; then beyond a strain of a few percent it bends over and finally crosses over to a stress plateau indicative of irreversible "dynamic yielding" or "plastic flow" on a local segmental scale. The corresponding yield stress, τ_y, increases with cooling. These basic features are in accord with experiment.[3−5] However, most stress−strain measurements exhibit an overshoot or local maximum (practical yield point) and an upturn at large deformation (strain hardening). The amplitude of the overshoot depends on the aged state of the sample. On the contrary, the flow or plateau stress is a function only of temperature and strain rate, not aging time or annealing protocol, which suggests a complete erasure of the thermo-mechanical history after yield.[3−5,33] Strain hardening is associated with anisotropic stretching of chains,[3−5,35] which is not included in the present theory. The aging/deaging and strain hardening phenomena are intentionally ignored in this initial work. The yield stress maximum feature can be avoided experimentally by performing rapid quenches or via mechanical pretreatment.

The stress−strain curves in Figure 3 can be very accurately (but not perfectly) superimposed onto a master curve by plotting in double-normalized manner (Figure 4). Stress is nondimensionalized by the yield plateau value, and strain is nondimensionalized by an empirically determined value, γ_y, chosen by optimizing the superposition. The extracted yield strain is several percent in magnitude and increases roughly in a linear manner with cooling depth, features in broad agreement with experiment.[3−5] Interestingly, the deduced γ_y values are quantitatively close to the a priori estimate of the effective yield strain defined in eq 22 (inset of Figure 4). Equation 22 shows $\tilde{\gamma}_y$ equals the product of the external strain rate and alpha relaxation time at yield, $\dot{\gamma}\tau_\alpha(\tau_y)$, which is clearly much less than unity. Hence, the theory *predicts* (not assumes) that in the plastic flow regime the material is "equilibrated" in the dynamical sense that the segmental relaxation time is short compared to the measurement time scale. However, the structure remains glasslike; i.e. S_0 is not its equilibrium value.

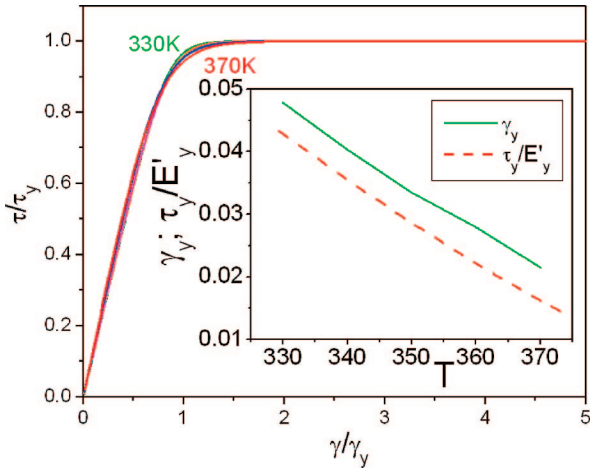

Figure 4. Superposition of the stress−strain curves in Figure 3 obtained by double normalization of scales by the plateau yield stress and an empirically determined yield strain. Inset: deduced yield strain, and the a priori computed effective yield strain of eq 22, as a function of temperature.

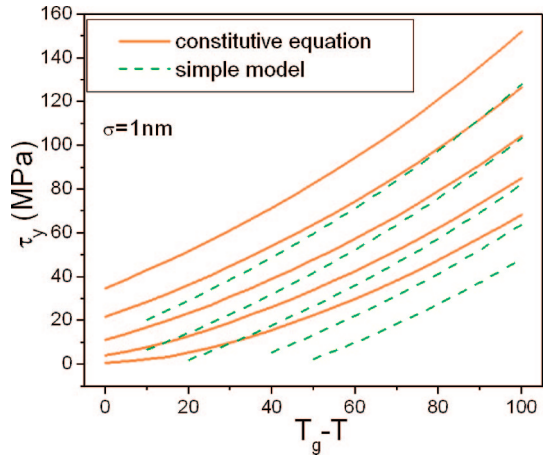

Figure 5. Dynamic yield stress as a function of cooling depth for strain rates (top to bottom) of 10^{-1}, 10^{-2}, 10^{-3}, 10^{-4}, and 10^{-5} Hz. Solid curves are the results based on the constitutive equation, and dashed curves are for the simple model of eq 2 studied in ref 32.

Figure 5 shows calculations of the dynamic yield stress as a function of temperature and the corresponding Eyring-like estimates based on eq 2. Results are shown for five strain rates that vary from 10^{-5} to 10^{-1} Hz. The two calculations of τ_y are quantitatively different, but all the qualitative features are the same. Overall, the results are in accord with observations.[3–5]

B. Isothermal Strain Rate Dependence. We now fix temperature and vary strain rate. The potential complication of deformation-induced sample heating sometimes encountered in real experiments is not considered. Figure 6 shows the strain rate dependence of the stress−strain response at a fixed temperature of 330 K ($T_g - T = 48$ K). Both the yield stress and yield strain increase modestly with strain rate. For example, as $\dot{\gamma}$ grows by 5 orders of magnitude, the yield stress increases by a factor of ∼5, and the yield strain increases from ∼3% to ∼11%. A very good master curve can again be achieved in the double-normalized representation of Figure 7. The empirically deduced yield strain, and its a priori estimate $\tilde{\gamma}_y \equiv \tau_y/E'(\tau_y)$, are quantitatively close, and both increase logarithmically with strain rate with a slight upward curvature at high rates (inset of Figure 7). These trends agree with many experiments on polymer glasses. The strain rate dependence of the dynamic plateau yield stress, and its simple analogue of eq 2, are

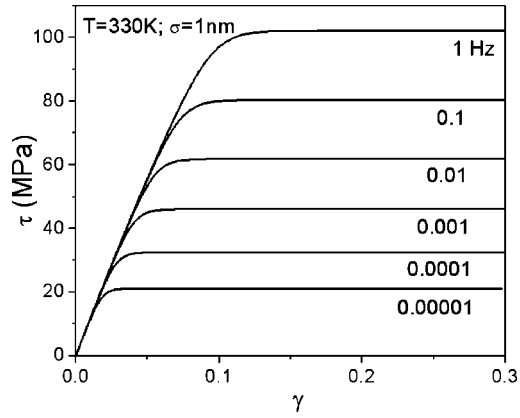

Figure 6. Stress−strain response for six values of strain rate at $T = 330$ K.

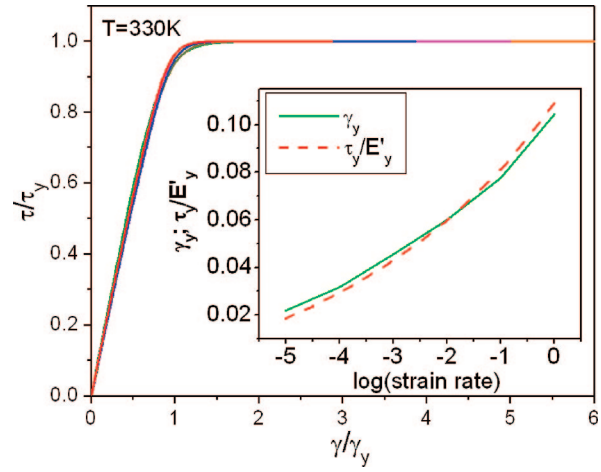

Figure 7. Superposition master plot for the five stress−strain curves in Figure 6 obtained by double normalization of the scales by plateau yield stress and an empirically determined yield strain. Inset: logarithmic strain rate dependence of the deduced yield strain and the a priori computed analogue of eq 22.

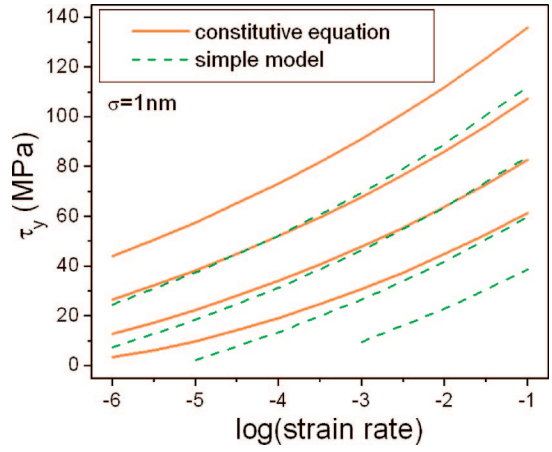

Figure 8. Dynamic plateau yield stress as a function of logarithmic strain rate for temperatures (top to bottom): 288, 308, 328, and 348 K. Solid curves are results based on the constitutive equation and dashed curves for the simple model of eq 2 studied in ref 32.

compared in Figure 8. Again, the overall trends agree and follow a roughly logarithmic growth with modest upward curvature at high rates.

It is of interest to know how the dynamic yield stress compares to its absolute analogue, τ_{abs}. Recall the latter is defined as the stress required to destroy the nonequilibrium free

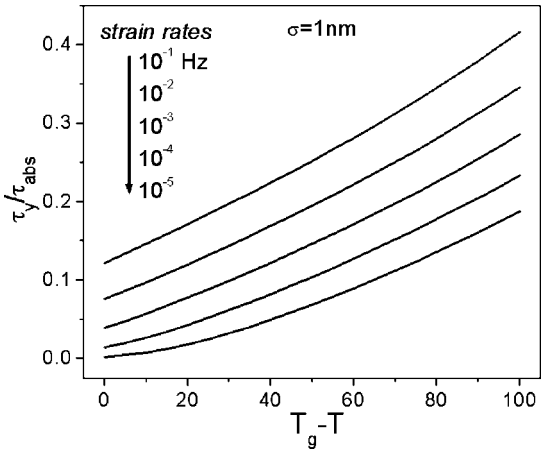

Figure 9. Dynamic yield stress reduced by the corresponding absolute yield stress as a function of degree of undercooling for five strain rates.

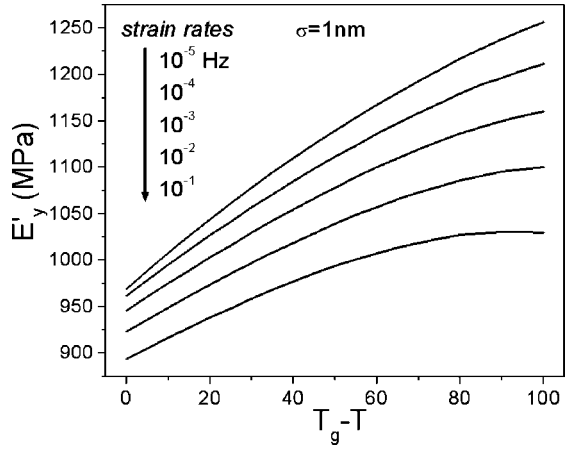

Figure 10. Young's modulus evaluated at the dynamic yield stress as a function of degree of undercooling for five strain rates.

energy barrier. Figure 9 presents plots of the ratio τ_y/τ_{abs} as a function of temperature for several strain rates. The ratio increases with cooling and strain rate but generally is much less than unity. Hence, we conclude that dynamic yielding corresponds to a stress-assisted, *but thermally driven*, activated barrier hopping process. As a consequence of $\tau_y \ll \tau_{abs}$ and $E'_y = E'(0)(1 - 2\tau_y/3\tau_{abs})$, the ratio $E'_y/E'(0)$ changes by only ~27% or much less. Since $E'(0)$ and $(1 - 2\tau_y/3\tau_{abs})$ vary oppositely with temperature, and $E'(0)$ increases by 50% at 100 K below T_g, we expect the elastic modulus *at* yield does not vary significantly with strain rate and temperature. This expectation is explicitly verified in Figure 10.

C. Quantitative Comparison to Experiments. The prior preliminary work[32] and present calculations both demonstrate that our theoretical predictions for the absolute magnitude, and temperature and strain rate dependences, of the yield stress and yield strain are in broad agreement with experiments on PMMA (and other) glasses. This is significant since there are essentially no fitting parameters in the nonlinear theory. We now compare more quantitatively with two specific experiments on PMMA glasses. The one parameter varied is the statistical segment length, σ. Given the characteristic ratio for atactic PMMA is ~9, the corresponding persistence and Kuhn lengths are ~0.75 and 1.35 nm, respectively.[38] With the exception of the modulus results in Figure 2, all PMMA calculations presented previously and in the present work have used $\sigma = 1$ nm. Varying σ simply scales the absolute magnitude of the stress, which is proportional to k_BT/σ^3.

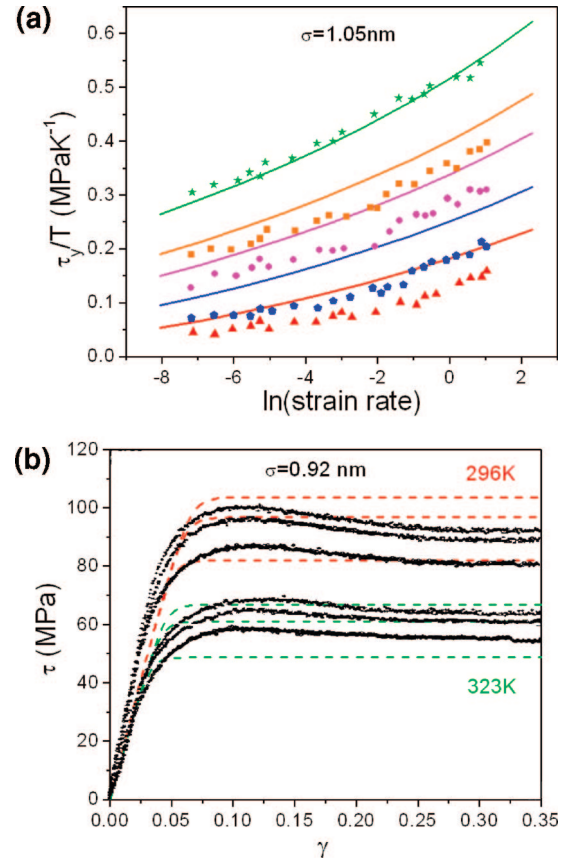

Figure 11. (a) Ratio of the dynamic yield (plateau flow) stress over temperature (MPa K^{-1}) as a function of the natural logarithm of strain rate for temperatures 97, 79, 67, 47, and 27 K below T_g (from top to bottom). Solid symbols are the PMMA experimental flow stress data measured at 20% strain.[62] The segment length is 1.05 nm. (b) Stress−strain curves at $T = 296$ and 323 K and three strain rates of 0.001, 0.0005, and 0.0001 Hz. The dashed lines are the theoretical results, and the dark coarse lines are the PMMA experimental data.[63] The statistical segment length is 0.92 nm.

The theoretical results are first compared with the plateau flow stress measurements on PMMA glass by Lee and Swallowe.[62] Their sample has a glass transition temperature of ~390 K, while $T_g = 378$ K in our theory. The comparison is performed at fixed degree of cooling below T_g, i.e., the same $\Delta T = T_g - T = 27$, 47, 67, 79, and 97 K, for strain rates in the range of 0.001−3 Hz. The same plotting format as employed in the experimental study is adopted, τ_y/T vs the *natural* logarithm of the strain rate. Results are shown in Figure 11a. Both the experimental data and the theoretical curves show a slightly nonlinear increase (curving up) of flow stress with logarithmic strain rate. Quantitative agreement is achieved for temperatures as low as 100 K below T_g by choosing the segment length $\sigma = 1.05$ nm, a reasonable value again intermediate between the persistence and Kuhn lengths for PMMA. Deviations are larger for higher temperature. However, given the essentially no adjustable parameter nature of the comparison of theory and experiment, we find the agreement to be satisfying.

We now compare the theoretical calculations with stress−strain measurements on quenched PMMA.[63] These experiments were performed well below the glass temperature at 296 and 323 K for strain rates of 10^{-4}, 5×10^{-4}, and 10^{-3} Hz. The results are shown in Figure 11b. Note there is very little stress overshoot in the experiments, indicating the rapid quenching protocol effectively avoids physical aging. Moreover, for strains up to 35% there is no indication of strain hardening. Encouraging agreement is achieved for the shape of the curves, and the yield

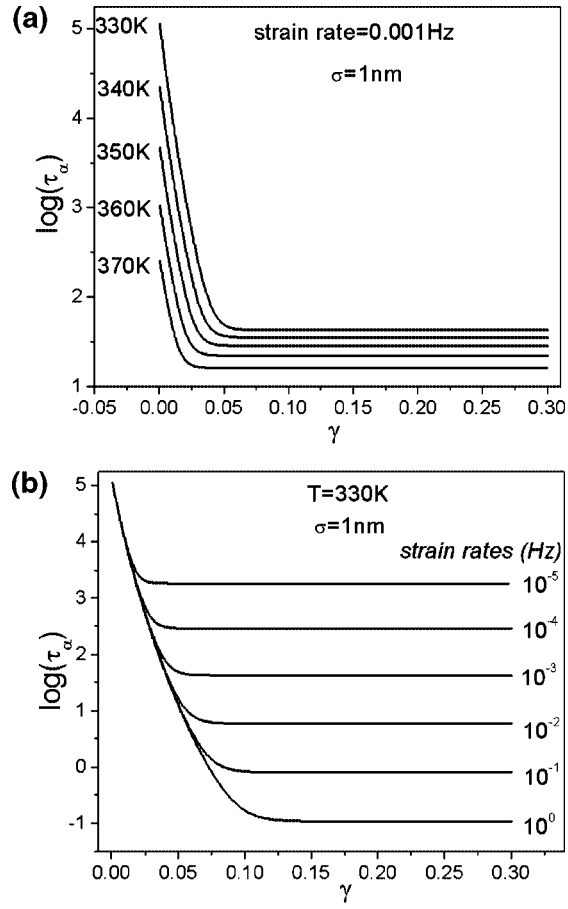

Figure 12. Logarithmic (base 10) alpha relaxation time as a function of strain (a) at a constant strain rate of 0.001 Hz for five temperatures and (b) at $T = 330$ K for six strain rates.

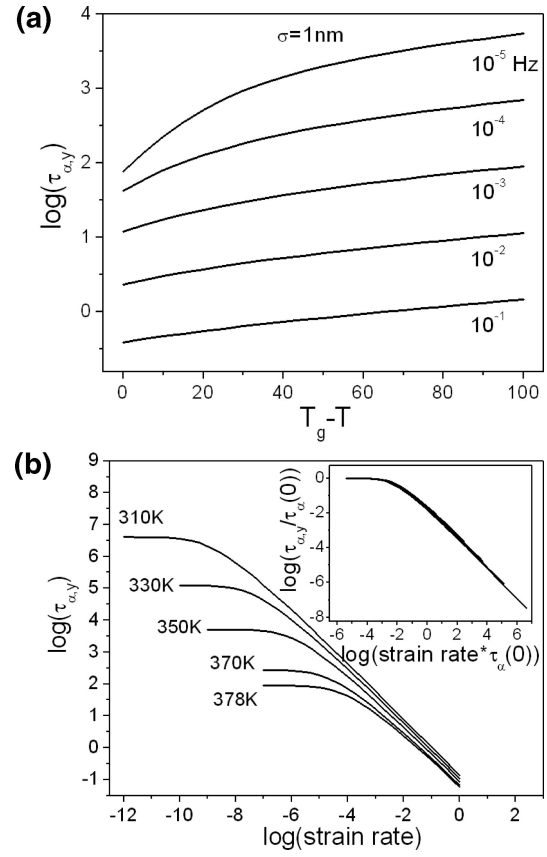

Figure 13. (a) Logarithmic relaxation time at the dynamic yield stress as a function of cooling depth for five strain rates. (b) A log−log plot of the relaxation time at yield as a function of strain rate for five temperatures. The inset shows its doubly normalized analogue where the low strain rate limit of $\tau_{\alpha,y}(\dot{\gamma}\rightarrow 0) = \tau_\alpha(0)$ is the common nondimensionalizing factor.

stresses and strains, by choosing the segment length $\sigma = 0.92$ nm. The latter value is again intermediate between the persistence and Kuhn lengths.

VI. Stress-Assisted Relaxation and Glass Melting

The dynamic yield stress follows from the self-consistent eq 21, and the alpha relaxation time plays a critical role in its determination. Deformation reduces the barrier and accelerates thermally induced activated barrier hopping, until a steady-state value, $\tau_\alpha(\tau_y)$, is achieved under plastic flow conditions. The acceleration of segmental relaxation under stress can be thought of as a deformation-induced reduction of the kinetic glass transition temperature.[32]

A. Alpha Relaxation Time Reduction. Figure 12 plots results for the segmental relaxation time as a function of strain at fixed strain rate. Qualitatively, the curves are inverted analogs of the stress−strain response. The relaxation time initially drops dramatically with strain in an exponential manner, before saturating at its plateau value. For example, at $T = 350$ K and $\dot{\gamma} = 10^{-3}$ Hz the relaxation time decreases by more than 2 orders of magnitude at $\gamma \sim 0.04$. This initial decrease with strain becomes more pronounced at lower temperatures or higher strain rates (Figure 12b). For example, in Figure 12a the quiescent alpha relaxation time varies from ∼300 to $\sim 10^5$ s as temperature is lowered from 370 to 330 K. However, in the plastic flow regime the variation of the alpha time is far less, from ∼15 to 50 s. The latter time scales are below the commonly employed definition of the kinetic glass transition of $\tau_\alpha(T_g) = 10^2-10^4$ s. Hence, our results provide fundamental theoretical support for the qualitative proposition[3,7] that stress-induced plastic flow or dynamic yielding can be thought of as a "devitrification" transition in a dynamical sense.

Figure 13 quantifies the temperature and strain rate dependences of the alpha relaxation time in the yield plateau regime. Figure 13a shows the relaxation time increases with cooling depth and decreasing strain rate. Moreover, the temperature sensitivity is clearly enhanced as the strain rate gets smaller. Considering the small variation with temperature of the elastic modulus at yield (Figure 10), the increase of yield stress with cooling (Figure 5) arises predominantly from an increase of the relaxation time at yield. Figure 13b presents our results in the format commonly adopted to describe "shear thinning" of complex fluids. The Newtonian plateau at low enough shear rates rolls over to an effective power law decrease of the relaxation time at a characteristic strain rate which increases with temperature. The apparent power-law exponent is ∼0.8−0.9 and gradually approaches unity in the ultrahigh strain rate limit. Such a crossover has been recently observed in simulations of the creep of a model polymer glass,[14,15] and there is general agreement between theory and simulation. Definitive experiments in the polymer glass state remain to be performed, and hence the results in Figure 13b serve as a prediction. In the inset of Figure 13b one sees that an excellent master curve is found based on nondimensionalizing the alpha time at yield and strain rate by the low strain rate plateau value $\tau_{\alpha,y}(\dot{\gamma}\rightarrow 0) = \tau_\alpha(0)$. Moreover, the onset of "shear thinning" occurs at small value of reduced strain rate, $\dot{\gamma}\tau_\alpha(0) \approx 10^{-3}-10^{-2}$.

B. Stress-Driven Devitrification and Liquid-like Domains. Figure 14 presents calculations of the dimensionless product of the relaxation time and strain rate, $\dot{\gamma}\tau_{\alpha,y}$, in the dynamic yield

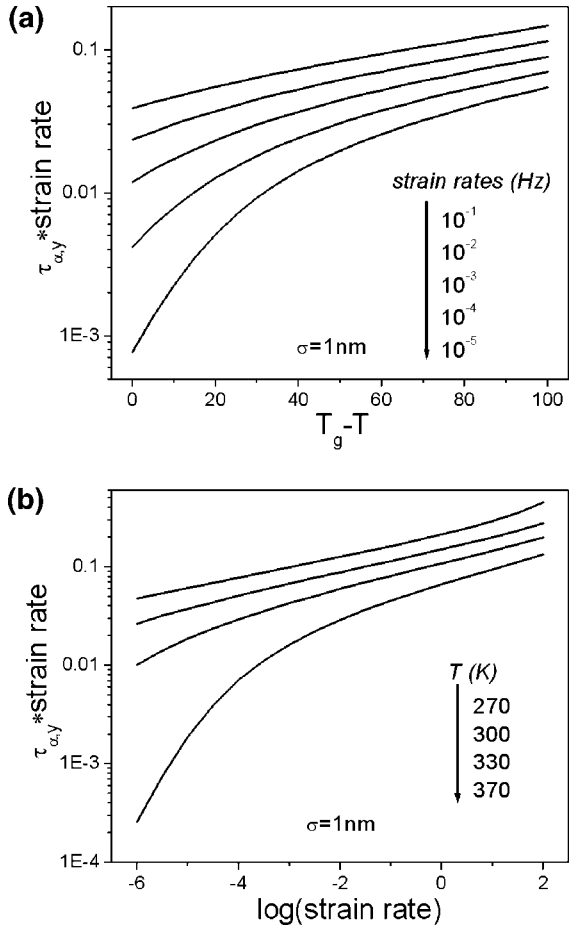

Figure 14. Product of the relaxation time at yield multiplied by the corresponding strain rate as a function of (a) cooling depth for five strain rates and (b) logarithmic strain rate for four temperatures.

regime as a function of temperature and $\dot{\gamma}$. In the Eyring picture this quantity is a constant. In contrast, our approach predicts $\tau_{\alpha,y}\dot{\gamma} = \tau_y/E'(\tau_y) \equiv \tilde{\gamma}_y$ is comparable to the yield strain (insets of Figures 4 and 7) and varies with temperature and strain rate. Figure 14 shows $\dot{\gamma}\tau_{\alpha,y}$ increases monotonically as temperature is lowered or strain rate increased. The overall form of the results are consistent with a recent simulation study of creep performed at one temperature.[15] The absolute magnitudes are also in accord with that simulation which find $\dot{\gamma}\tau_{\alpha,y} \sim 0.1-0.3$ at high strain rates.

There are other interesting trends in Figure 14 worth pointing out. At low temperatures, a weak dependence of $\dot{\gamma}\tau_{\alpha,y}$ on the cooling depth is predicted which appears to be insensitive to strain rate to a first approximation (Figure 14a). Similarly, at high strain rates an apparent power law growth of $\dot{\gamma}\tau_{\alpha,y}$ with strain rate occurs with a small effective exponent that is insensitive to temperature. For example, at $T = 300$ K the product changes only from ~0.07 to ~0.3 when the strain rate increases about 5 orders of magnitude. We note that the high strain rate and/or low temperature regime is characterized by highly inefficient thermally activated hopping under quiescent conditions in the sense $\tau_\alpha(\tau = 0;T)\dot{\gamma} \gg 1$. On the other hand, at high temperature and/or low strain rates $\dot{\gamma}\tau_{\alpha,y}$ can be much smaller and is much more temperature sensitive. This is the regime where $\tau_\alpha(\tau = 0;T)\dot{\gamma}$ is not very large.

Despite the rich dependence of $\dot{\gamma}\tau_{\alpha,y}$ on temperature and strain rate, we find that for all cases examined in Figure 14, which cover the typical ranges of temperature and $\dot{\gamma}$ studied experimentally, this quantity is significantly less than unity. Such a prediction seems highly nontrivial. It has the important implication that on the experimental time scale the system is *dynamically* equilibrated on the segmental length scale probed by the alpha relaxation process.

Finally, the quantitative aspects of the results in Figure 14 have two additional interesting implications. First, the picture of a glass consisting of kinetically fluidized "nanodomains" in the yield stress plateau regime has been suggested.[56,64] Polymers have a spectrum of normal modes that span the range from segmental to macromolecular length scales.[65] For unentangled chains, or entangled polymers on length scales below the entanglement length (~8 nm for PMMA), the Rouse model is a zeroth-order description of how the chain relaxation time depends on the spatial scale $\xi_p \equiv \sigma(N/p)^{1/2}$, where p is the mode index. If τ_α is interpreted as the most local segment relaxation time ($p = N$), then the relaxation time on the length scale ξ_p is given $\tau_p/\tau_\alpha = (N/p)^2$. Qualitatively, the system will be liquid- or rubber-like inside a critical length scale $\xi_c \equiv \xi_{p=p_c}$ defined by $\dot{\gamma}\tau_{p=p_c} = 1$. Since we predict $\dot{\gamma}\tau_{\alpha,y} \sim 0.01-0.1$ over a wide range of temperature and strain rates, liquid-like domains are estimated to exist in the glass *under* dynamic yielding conditions on a length scale $\xi_c \simeq (3-10)\sigma \sim 3-10$ nm. This estimate seems consistent with very recent scattering experiments on PMMA glasses.[56]

Second, the existence of liquid-like domains on the experimental (mechanical) time scale has implications for over what length scales polymer glass deformation is affine. On scales beyond ξ_c one expects based on the Rouse model that relaxation times will be too slow to produce significant equilibration on the measurement time scale. Hence, the polymer glass should deform affinely over distances greater than $\sim\xi_c$. This admittedly rough analysis is consistent with X-ray scattering studies of the crossover length scale for affine behavior of highly deformed PMMA glasses[56] and also solid-state NMR studies of the length scale beyond which the "pseudo-affine" model of rigidly reorienting chain units describes the measured orientational order parameter.[5,66]

VII. Summary and Discussion

We have built on prior force-level barrier hopping theories for the quiescent and stress-assisted thermally activated segmental dynamics of polymer melts[24–26] and glasses[30–32] to construct a general constitutive equation description of nonlinear mechanics at a generalized Maxwell model level. The theory has been illustrated via numerical calculations for PMMA glass under constant strain rate conditions. The key physics resides in a deformation-dependent elastic modulus and alpha relaxation time which are determined by a segment-displacement-dependent effective free energy which quantifies the transient localization process.

Detailed calculations of the temperature and strain rate dependence of the stress−strain curves, yield stress, and yield strain for PMMA glass, a representative amorphous plastic, have been presented. The strain rate dependences are all logarithmic with upward deviations at very high rates. Yield stresses grow roughly linearly as temperature is lowered. The dynamic yield stress is generally much smaller than its "absolute" analogue which corresponds to complete destruction of the effective free energy barrier and purely mechanically driven flow. Hence, (local) plastic flow or dynamic yielding is a stress-assisted, but thermally driven, activated barrier hopping process. Stress−strain curves at different temperatures and strain rates can be collapsed onto a master curve based on nondimensionalization of stress by its plateau yield value and reduction of strain by an effective critical value. The latter is very nearly equal to an a priori computed effective yield strain given by the ratio of the stress to elastic modulus *at yield*. Quantitative calculations of the PMMA stress−strain response in the glass as a function of

temperature and strain rate are in good agreement with several experiments based on essentially no adjustable parameters.

We note that the constitutive equation developed in section IV is new. It is meant to describe segment scale glassy dynamics, not macromolecular scale entangled dynamics, well above T_g. In this regard, we point out that the empirical Cox−Merz rule[67] which equates the dependence of the viscosity on shear rate to the frequency-dependent linear dynamic modulus is not obeyed, and our constitutive equation differs in fundamental ways from other approaches.[68]

Calculations that address how stress and strain reduce the segmental relaxation time, leading to a type of deformation-induced "glass melting", have been presented. In the dynamic yielding regime the segmental relaxation time is predicted to generally be much shorter than the inverse strain rate. Hence, our results provide fundamental theoretical support for the qualitative idea that stress-induced plastic flow can be thought of as a "devitrification" transition in a dynamical sense. The segmental relaxation time in the yielding regime displays a "shear thinning" type of dependence on strain rate, and effective power law decay with strain rate is predicted with an exponent slightly smaller than unity under low temperature and/or high strain rate conditions.

The theory as presently formulated can be immediately applied to compute single and multistep creep and creep recovery, step strain, and oscillatory strain mechanical measurements. Results will be reported in a future publication.

Our approach as presented here is meant for segmental dynamics below T_g and invokes several simplifications. First, dynamic heterogeneity effects associated with nonexponential relaxation have been ignored. Although an important quantitative issue under quiescent conditions, at high stresses, especially in the plastic flow regime, such dynamical fluctuation effects may be considerably less important. For example, recent simulations of the creep of polymer glasses,[15] and experiments on glassy colloids at high shear rates,[21] suggest local relaxation processes are nearly single exponential or Maxwellian as assumed in our present formulation. Future work will explore the consequences of nonexponential relaxation on the stress−strain response, but preliminary calculations suggest all qualitative features are unaffected. Second, the coupled effects of physical aging and deformation-induced "rejuvenation"[2,3,33] have been ignored. We have previously developed a predictive theory for the physical aging process under quiescent conditions.[31] Ongoing work is aimed at generalizing this to the nonlinear regime, along with the formulation of a theory for how deformation enhances dynamics via increasing the amplitude of density fluctuations. The latter can result in a form of "erasure" of the aging process and the attainment of a new nonequilibrium steady state. The fascinating, but poorly understood, phenomenon of strain hardening at large deformation[3–5,35] where polymer chains are strongly stretched or compressed is under study based on accounting for how anisotropic chain conformations modify density fluctuations and caging forces.[69] Finally, in principle, the theory can be applied to the $T > T_g$ fully molten state. However, in this regime chain scale dynamics dominates the observable low frequency mechanical response. Hence, the present theory must be merged with chain dynamics theories of unentangled and entangled polymer liquids, a challenge that remains for the future.

Acknowledgment. This work was supported by the National Science Foundation as NIRT project 0505840. Helpful discussions with Mark Ediger, Juan dePablo, and Rob Riggleman are gratefully acknowledged.

References and Notes

(1) Angell, C. A.; Ngai, K. L.; McKenna, G. B.; McMillan, P. F.; Martin, S. W. *J. Appl. Phys.* **2000**, *88*, 3113.
(2) McKenna, G. B. *J. Phys.: Condens. Matter* **2003**, *15*, S737.
(3) Meijer, H. E. H.; Govaert, L. E. *Prog. Polym. Sci.* **2005**, *30*, 915.
(4) Haward, R. N.; Young, R. J. *The Physics of Glassy Polymers*; Chapman and Hall: London, 1997.
(5) Ward, I. M.; Hadley, D. W. *Introduction to Mechanical Properties of Solid Polymers*; Wiley and Sons: New York, 1993.
(6) Arruda, E. M.; Boyce, M. C.; Jayachandran, R. *Mech. Mater.* **1995**, *19*, 193.
(7) van Melick, H. G. H.; Govaert, L. E.; Raas, B.; Nauta, W. J.; Meijer, H. E. H. *Polymer* **2003**, *44*, 1171.
(8) Mulliken, A. D.; Boyce, M. C. *Int. J. Solids Struct.* **2006**, *43*, 1331.
(9) Palm, G.; Dupaix, R. B.; Castro, J. *J. Eng. Mater. Technol.* **2006**, *128*, 559.
(10) Yee, A.; Bankert, R. J.; Ngai, K. L.; Rendell, R. W. *J. Polym. Sci., Polym. Phys.* **1998**, *26*, 2463.
(11) Loo, L.; Cohen, R.; Gleason, K. *Science* **2000**, *288*, 116.
(12) Lee, H. N.; Pang, K.; Swallen, S. F.; Ediger, M. D. *J. Chem. Phys.* **2008**, *128*, 134902.
(13) Warren, M.; Rottler, J. *Phys. Rev. E* **2007**, *76*, 031802.
(14) Riggleman, R.; Lee, H. N.; Ediger, M. D.; dePablo, J. J. *Phys. Rev. Lett.* **2007**, *99*, 215501.
(15) Riggleman, R.; Schweizer, K. S.; dePablo, J. J. *Macromolecules* **2008**, *41*, 4969.
(16) (a) Capaldi, F. M.; Boyce, M. C.; Rutledge, G. C. *Phys. Rev. Lett.* **2002**, *89*, 175505. (b) *Polymer* **2004**, *45*, 1391.
(17) Lyulin, A. V.; Balabaev, N. K.; Mazo, M. A.; Michels, M. A. J. *Macromolecules* **2004**, *37*, 8785.
(18) Lyulin, A. V.; Vorelaars, B.; Mazo, M. A.; Michels, M. A. J. *Europhys. Lett.* **2005**, *71*, 618.
(19) Eyring, H. *J. Chem. Phys.* **1936**, *4*, 283.
(20) (a) Rottler, J.; Robbins, M. O. *Phys. Rev. Lett.* **2005**, *95*, 225504. (b) *Phys. Rev. E* **2003**, *68*, 011507.
(21) Besseling, R.; Weeks, E. R.; Schofeld, A. B.; Poon, W. C. K. *Phys. Rev. Lett.* **2007**, *99*, 028301.
(22) (a) Yamamoto, R.; Onuki, A. *Phys. Rev. E* **1998**, *58*, 3515. (b) Miyazaki, K.; Yamamoto, R.; Reichman, D. R. *Phys. Rev. E* **2004**, *70*, 011501.
(23) Foss, D. R.; Brady, J. F. *J. Fluid. Mech.* **1999**, *401*, 243.
(24) Schweizer, K. S.; Saltzman, E. J. *J. Chem. Phys.* **2004**, *121*, 1984.
(25) Saltzman, E. J.; Schweizer, K. S. *J. Chem. Phys.* **2004**, *121*, 2001.
(26) Saltzman, E. J.; Schweizer, K. S. *J. Phys.: Condens. Matter* **2007**, *19*, 205123.
(27) Schweizer, K. S.; Saltzman, E. J. *J. Chem. Phys.* **2003**, *119*, 1181.
(28) Schweizer, K. S. *J. Chem. Phys.* **2005**, *123*, 244501.
(29) (a) Saltzman, E. J.; Schweizer, K. S. *J. Chem. Phys.* **2006**, *125*, 044509. (b) *Phys. Rev. E* **2006**, *74*, 061501.
(30) Chen, K.; Schweizer, K. S. *J. Chem. Phys.* **2007**, *126*, 014904.
(31) Chen, K.; Schweizer, K. S. *Phys. Rev. Lett.* **2007**, *98*, 167802.
(32) Chen, K.; Schweizer, K. S. *Europhys. Lett.* **2007**, *79*, 26006.
(33) Struick, L. C. E. *Physical Aging in Amorphous Polymers and Other Materials*; Elsevier: Amsterdam, 1978.
(34) (a) Ediger, M. D. *Annu. Rev. Phys. Chem.* **2000**, *51*, 99. (b) Richert, R. *J. Phys.: Condens. Matter* **2002**, *14*, R703.
(35) (a) Hoy, R.; Robbins, M. O. *J. Polym. Sci., Polym. Phys.* **2006**, *44*, 3487. (b) *Phys. Rev. Lett.* **2007**, *99*, 117801. (c) *Phys. Rev. E* **2008**, *77*, 031801.
(36) Novikov, V. N.; Sokolov, A. P. *Phys. Rev. E* **2003**, *67*, 031507.
(37) (a) Lodge, T. P.; McLeish, T. C. B. *Macromolecules* **2000**, *33*, 5278. (b) Inoue, T.; Osaki, K. *Macromolecules* **1996**, *29*, 1595.
(38) Mattice, W. L.; Suter, U. W. *Conformational Theory of Large Molecules*; Wiley: New York, 1994.
(39) Stillinger, F. H.; Debenedetti, P. G.; Sastry, S. *J. Chem. Phys.* **1998**, *109*, 3983.
(40) (a) Roe, R. J.; Curro, J. J. *Macromolecules* **1983**, *16*, 428. (b) Roe, R. J. *J. Chem. Phys.* **1983**, *79*, 936. (c) Roe, R. J. *Macromolecules* **1981**, *14*, 1586.
(41) (a) Wendorff, J. H. *J. Polym. Sci., Polym. Lett. Ed.* **1979**, *17*, 765. (b) Wendorff, J. H.; Fischer, E. W. *Kolloid Z. Z. Polym.* **1973**, *251*, 876. (c) Fischer, E. W. *J. Macromol. Sci., Phys.* **1976**, *B12*, 41.
(42) (a) Jain, S. C.; Simha, R. *Macromolecules* **1982**, *15*, 1522. (b) Simha, R.; Jain, S. C.; Jamieson, A. M. *Macromolecules* **1982**, *15*, 1517. (c) Balik, C. M.; Jamieson, A. M.; Simha, R. *Colloid Polym. Sci.* **1982**, *260*, 477.
(43) (a) Floudas, G.; Pakula, T.; Fischer, E. W. *Macromolecules* **1994**, *27*, 917. (b) Floudas, G.; Pakula, T.; Stamm, M.; Fischer, E. W. *Macromolecules* **1993**, *26*, 1617.
(44) (a) Ruland, W. *Prog. Colloid Polym. Sci.* **1975**, *57*, 192. (b) *Pure Appl. Chem.* **1977**, *49*, 905. (c) Rathje, J.; Ruland, W. *Colloid Polym. Sci.* **1976**, *254*, 358.

(45) (a) Faivre, A.; David, L.; Vassoile, R.; Vigier, G.; Etienne, S.; Geissler, E. *Macromolecules* **1996**, *29*, 8387. (b) David, L.; Vigier, G.; Etienne, S.; Faivre, A.; Soles, C. L.; Yee, A. F. *J. Non-Cryst. Solids* **1998**, *383*, 235–237.
(46) (a) Debenedetti, P. G.; Stillinger, F. H. *Nature (London)* **2001**, *410*, 259. (b) Stillinger, F. H. *Science* **1995**, *267*, 1935.
(47) (a) Thurau, C. T.; Ediger, M. D. *J. Chem. Phys.* **2003**, *118*, 1996. (b) *J. Chem. Phys.* **2002**, *116*, 9089.
(48) O'Connell, P. A.; McKenna, G. B. *J. Chem. Phys.* **1999**, *110*, 11054.
(49) Simon, S. L.; Sobieski, J. W.; Plazek, D. J. *Polymer* **2001**, *42*, 2555.
(50) Schlosser, E.; Schonhals, A. *Polymer* **1991**, *32*, 2135.
(51) (a) Alegria, A.; Guerrica-Echevarria, E.; Telleria, I.; Colmenero, J. *Phys. Rev. B* **1993**, *47*, 14857. (b) Goitiandia, L.; Alegria, A. *J. Chem. Phys.* **2004**, *121*, 1636.
(52) Ehlich, D.; Sillescu, H. *Macromolecules* **1990**, *23*, 1600.
(53) (a) Kobelev, V.; Schweizer, K. S. *Phys. Rev. E* **2005**, *71*, 021401. (b) *J. Chem. Phys.* **2005**, *123*, 164902.
(54) Saltzman, E. J.; Yatsenko, G.; Schweizer, K. S. *J. Phys.: Condens. Matter* **2008**, 000
(55) Our precise numerical results are sensitive to the coarse graining scale (segment length σ) and stress-displacement prefactor, c. Estimates of the latter are discussed in ref 53. In our present and prior calculations we employ $c = (\pi\rho\sigma^3/6)^{-2/3}$ and $\sigma = 1$ nm. If these quantities are changed, then all stress values change multiplicatively by the factor $(1\ \text{nm}/\sigma)^3(1.63/c)$.
(56) (a) Casa, F.; Alba-Simionesco, C.; Lequeux, F.; Montes, H. *J. Non-Cryst. Solids* **2006**, *352*, 5076. (b) *Macromolecules* **2008**, *41*, 860.
(57) Dettemnaier, M.; Maconnachie, A.; Higgins, J. S.; Kausch, H. H.; Nguyen, T. Q. *Macromolecules* **1996**, *19*, 773.
(58) Lacks, D. J. *Phys. Rev. Lett.* **2001**, *87*, 225502.
(59) Sollich, P.; Lequeux, F.; Hebraud, P.; Cates, M. *Phys. Rev. Lett.* **1997**, *78*, 2020.
(60) Seitz, J. T. *J. Appl. Polym. Sci.* **1993**, *49*, 1331.
(61) Scherer, G. W. *Relaxation in Glass and Composites*; John Wiley and Sons: New York, 1986.
(62) Lee, S. F.; Swallowe, G. M. *J. Mater. Sci.* **2006**, *41*, 6280.
(63) Hasan, O. A.; Boyce, M. C.; Li, X. S.; Berko, S. *J. Polym. Sci., Polym. Phys.* **1993**, *31*, 185.
(64) Oleynik, E. F.; Salamatina, O. B.; Rudnev, S. N.; Shenogin, S. V. *Polym. Sci.* **1993**, *35*, 1532.
(65) Rubinstein, M.; Colby, R. H. *Polymer Physics*; Oxford Press: Oxford, 2003.
(66) (a) Wendlandt, M.; van Beek, G. D.; Suter, U. W.; Meier, B. H. *Macromolecules* **2005**, *38*, 8372. (b) Ward, I. M. *Phys. Scr.* **1994**, *T55*, 224.
(67) Cox, W. P.; Merz, E. H. *J. Polym. Sci.* **1958**, *28*, 619.
(68) Dyre, J. C. *Rheol. Acta* **1990**, *29*, 145.
(69) Oyerokun, F. T.; Schweizer, K. S. *J. Chem. Phys.* **2005**, *123*, 224901.

MA800778V